Soft-mode behavior and incipient ferroelectricity in $Na_{1/2}Bi_{1/2}Cu_3Ti_4O_{12}$

Matthew C. Ferrarelli,[1] Dmitry Nuzhnyy,[2] Derek C. Sinclair,[1] and Stanislav Kamba[2]

[1]*Department of Engineering Materials, University of Sheffield, Sir Robert Hadfield Building, Mappin Street, Sheffield S1 3JD, United Kingdom*

[2]*Institute of Physics, Academy of Sciences of the Czech Republic, Na Slovance 2, 182 21 Prague 8, Czech Republic*

The correlation between crystal structure and intrinsic dielectric properties of the unusual cubic perovskite-related family of compounds $ACu_3Ti_4O_{12}$, where A=Ca, Cd, $La_{2/3}$, $Bi_{2/3}$, $Na_{1/2}La_{1/2}$, $Na_{1/2}Bi_{1/2}$, etc., (space group $Im\bar{3}$) has been a controversial topic for several years, especially for the most studied member of the family $CaCu_3Ti_4O_{12}$ (CCTO). $Na_{1/2}Bi_{1/2}Cu_3Ti_4O_{12}$ (NBCTO) is isostructural with CCTO and retains centrosymmetric and cubic symmetry (space group $Im\bar{3}$) down to 4 K. NBCTO ceramics exhibit high intrinsic relative permittivity of ~145 at 300 K that rises on cooling and levels off below ~50 K with a value of ~260 at 10 K without any signature of a structural transition. Such behavior is a typical feature of incipient ferroelectrics such as the perovskite $CaTiO_3$. Infrared and terahertz spectroscopy on NBCTO ceramics are presented and reveal a room-temperature soft polar optic mode at ~34 cm^{-1} that softens on cooling and is responsible for the temperature dependence of the relative permittivity. The temperature dependence of the soft-mode frequency obeys the Barrett formula with the onset of quantum fluctuations T_1 occurring near 85 K and a hypothetical Curie temperature T_0 of ~−155 K. A fitted vibrational zero-point energy $(k_BT_1)/2$ is in good agreement with the measured soft-mode frequency. The crystal structure-intrinsic dielectric properties of NBCTO and possibly all cubic $ACu_3Ti_4O_{12}$ phases are, therefore, consistent with that of other untilted/tilted TiO_3-based centrosymmetric perovskites such as $CaTiO_3$ and $SrTiO_3$. The "so-called" giant permittivity values of >1000 reported for CCTO, NBCTO, and related phases from radio-frequency capacitance measurements near room temperature are an extrinsic effect associated with the semiconducting nature of these materials, as opposed to an intrinsic effect associated with their rather unusual perovskite-type crystal structure.

PACS number(s): 77.84.Bw, 78.20.−e, 78.30.Am, 77.22.Ch

I. INTRODUCTION

Incipient ferroelectrics are materials that exhibit high permittivity ε' that rises rather steeply on cooling toward 0 K but saturates at low temperatures due to quantum fluctuations. The Barrett equation below is often used to fit the temperature T dependence of relative permittivity ε_r for incipient ferroelectrics.[1] This equation is defined as

$$\varepsilon_r = \frac{M}{\left(\dfrac{T_1}{2}\right)\coth\left(\dfrac{T_1}{2T}\right) - T_0} + A, \qquad (1)$$

where M is a constant, T_1 is the crossover temperature from low-temperature quantum to higher temperature classic paraelectric behavior, T_0 is the expected (or hypothetical) Curie temperature, and A is the permittivity at the high-frequency limit. For $T \gg T_1$, the term $(T_1/2)\coth(T_1/2T)$ approaches T and the equation reduces to the modified Curie-Weiss (C-W) law used to describe the temperature dependence of ε_r for conventional ferroelectrics in the paraelectric state with M becoming equivalent to the Curie Constant, C. For $T \ll T_1$, quantum effects become important and ε_r deviates from the simple Curie-Weiss law. In many cases T_0 is <0 K, i.e., the material does not undergo a ferroelectric phase transition at any finite temperature, whereas in other cases T_0 is finite but is <T_1, i.e., quantum fluctuations break the long-range ferroelectric order and stabilize the paraelectric state.

Classic examples of incipient ferroelectrics are based on ABO_3 perovskites containing a polarizable d^0 cation such as Ti^{4+}, Ta^{5+}, or Nb^{5+} on the B site and an untilted/tilted network of three-dimensional corner-sharing BO_3 units. Examples with $T_0 > 0$ K include $SrTiO_3$ (T_0=38 K) (Ref. 2) and $KTaO_3$ (T_0=13.1 K) (Ref. 3) whereas $CaTiO_3$ (T_0= −111 K),[4] $EuTiO_3$ (T_0=−221 K),[5] $Na_{1/2}Ln_{1/2}TiO_3$ [T_0= −770−(−2400) K],[6] where Ln=La, Pr, Nd, Sm, or Eu, and a pyrochlore-structured compound $Pb_{1.83}Mg_{0.29}Nb_{1.71}O_{6.39}$ (T_0=−167 K) (Ref. 7) are examples where $T_0 < 0$ K. Cases where T_0 is positive but less than T_1, e.g., $SrTiO_3$ (T_1 ~ 84 K) and $KTaO_3$ (T_1=56.9 K) are sometimes referred to as quantum paraelectrics, but such materials can be classified as a subset of incipient ferroelectrics.

The dielectric and the structural properties of incipient ferroelectrics can be very sensitive to impurities with the inclusion of small amounts of dopants causing relaxor or ferroelectric behavior. For example, x=0.002 of Ca in $Sr_{1-x}Ca_xTiO_3$ induces relaxor ferroelectric behavior[8] with long-range ferroelectric order achieved for $x > 1\%$.[9] Furthermore, 2% Mn doping on the Sr site of $SrTiO_3$ produces magnetoelectric multiglass properties, i.e., dipolar and spin-glass properties are simultaneously observed at low temperatures.[10] Theoretical and experimental work on incipient ferroelectrics are well reviewed in Refs. 11 and 12.

The increase in ε_r on cooling for incipient ferroelectrics is due to softening of the lowest frequency polar optical phonon (the "so-called" soft mode), but where freezing of the mode, i.e., a ferroelectric state, is never attained. The quantum fluctuations prevent excessive phonon softening and the

soft-mode frequency ω_{SM} saturates at a finite low value according to a modified Barrett formula[13]

$$\omega_{SM} = \sqrt{B\left[\left(\frac{T_1}{2}\right)\coth\left(\frac{T_1}{2T}\right) - T_0\right]}, \qquad (2)$$

where B is a constant.

Recently there has been much interest in the dielectric properties of a family of $AA'_3Ti_4O_{12}$ compounds, where A = Ca, Cd, La$_{2/3}$, Bi$_{2/3}$, Na$_{1/2}$La$_{1/2}$, Na$_{1/2}$Bi$_{1/2}$, etc., and A' = Cu^{2+}.[14–20] These $ACu_3Ti_4O_{12}$ compounds are part of a larger family with the general formula $AA'_3B_4O_{12}$, where A = Na, Ca, Sr, La, Bi, etc., A' = Cu or Mn, and B = Ti, Ru, Mn, Fe, Sn, V, or Ge (Refs. 16 and 21–25) and can also exhibit magnetic order. They can all be described as cubic, perovskite-related phases, space group $Im\bar{3}$, with 1:3 ordering of the A and Cu or Mn ions on the A and A' sites, respectively, and Ti, Ru, Mn, Fe, Sn, V, or Ge ions occupying the octahedral B sites. The octahedral units are in phase tilted ($a^+a^+a^+$, Glazer notation) with a large tilt angle, >22.4°. All of the $ACu_3Ti_4O_{12}$ compounds exhibit giant permittivity (>1000) at radio frequencies (rf) near room temperature.[14,16,20] Although interpretation of this giant permittivity has been controversial for a number of years, it is now generally accepted that they are semiconductors and the giant permittivity is an extrinsic effect, as opposed to an intrinsic effect associated with the rather unusual perovskite-related crystal structure. In the case of A = Ca (CCTO) and Na$_{1/2}$Bi$_{1/2}$ (NBCTO), a combination of impedance spectroscopy (IS) and local/surface probe techniques have been used to show ceramics are electrically heterogeneous, containing semiconducting grains (<100 Ω cm at 300 K) and insulating grain boundaries (>1 MΩ cm at 300 K).[17–20,26–28] The high apparent permittivity near room temperature in $ACu_3Ti_4O_{12}$ ceramics can, therefore, be explained as an internal barrier layer capacitance (IBLC) or a Maxwell-Wagner effect. The effect has also been observed for single crystals of CCTO where grain boundaries should be absent and therefore the IBLC mechanism cannot be the source of the extrinsic permittivity.[15] By applying metal electrodes with different work functions to CCTO single crystals we have used IS to show the giant permittivity effect in this case to be associated with non-Ohmic electrode contacts to semiconducting crystals.[29]

Based on their IR studies, Homes *et al.*[15] reported that the intrinsic ε_r coming from polar phonons in CCTO increases from ~75 (at 300 K) to ~115 at 10 K. These values are consistent with other reports of ε_r at low temperature using low frequency, <1 GHz, measurements.[19,30] Due to the semiconducting nature of these samples only limited data, below 100 K, can be obtained from low-frequency measurements. NBCTO ceramics exhibit a much larger and steeper increase in ε_r on cooling, reaching ε_r ~ 260 at 10 K (see Ref. 19 or 1 MHz rf data set in Fig. 1). Recently, we reported that Mn doping (~2–6 at %) on the Cu site is effective in suppressing the conductivity in these materials by at least 6 orders of magnitude at room temperature and this allowed ε_r to be measured over a much wider temperature range using rf measurements.[31–33] ε_r of Mn-doped CCTO increased with
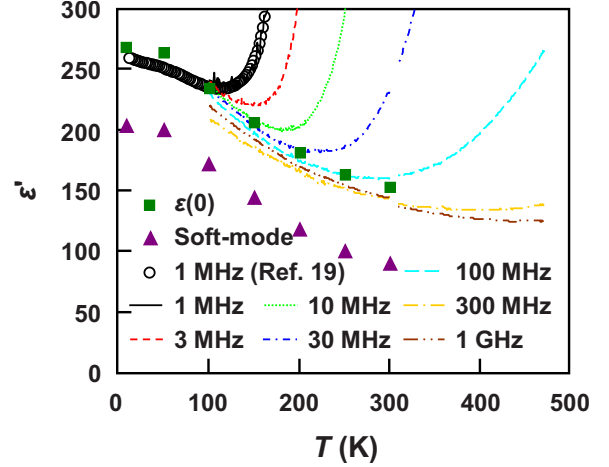
FIG. 1. (Color online) Temperature dependence of ε' at selected fixed frequencies for NBCTO ceramics. The contribution of the soft mode (filled purple triangles) and the combined phonon and electronic contributions $\varepsilon(0)$ (filled green squares) to ε' are added for comparison.

decreasing temperature and obeyed the C-W law over the range ~60–300 K with an expected T_0 of −383 K.[32] Deviation from C-W behavior was observed below 60 K but we were unable to obtain a sensible fit of the ε_r data to the Barrett equation. This may have been due to the presence of a small volume fraction (~2–5 %) of CaTiO$_3$ as a secondary phase in our samples. In the case of Mn-doped NBCTO, ε_r was ~140 at 320 K, increased with decreasing temperature and saturated at a value of ~240 below ~50 K. A C-W plot of $1/\varepsilon_r$ versus T showed linear behavior between ~140 and 320 K with T_0 ~ −246 K.[33] The ε_r data (at 100 kHz) were fitted to the Barrett equation, see Fig. 2(b) in Ref. 33, with M = 39306(5862) K^{-1}, T_1 = 255(12) K, T_0 = −79(27) K, and A = 50(9). The value of T_1 was higher than expected and is too high compared to that obtained from other incipient ferroelectrics such as CaTiO$_3$ and SrTiO$_3$. This was attributed to the influence of leakage conductivity on the rf measurements for Mn-doped NBCTO. Nevertheless, based on these results we have suggested NBCTO, and possibly other related $ACu_3Ti_4O_{12}$ phases such as CCTO, may exhibit incipient ferroelectricity, however, higher frequency permittivity measurements to fully eliminate the influence of leakage conductivity and infrared (IR) and terahertz (THz) spectroscopy measurements to probe the contribution of lattice vibrations to ε_r are required to confirm this suggestion.

Here we present results from a high-frequency spectroscopic study on undoped NBCTO ceramics that reveal evidence for a temperature-dependent soft mode (ω_{SM} ~ 20–35 cm^{-1}) whose softening saturates below ~50 K and obeys the modified Barrett equation [Eq. (2)]. This confirms incipient ferroelectricity to occur in this compound.

II. EXPERIMENTAL

The conditions for preparation of NBCTO powders and ceramics are reported elsewhere.[19] High-frequency permit-
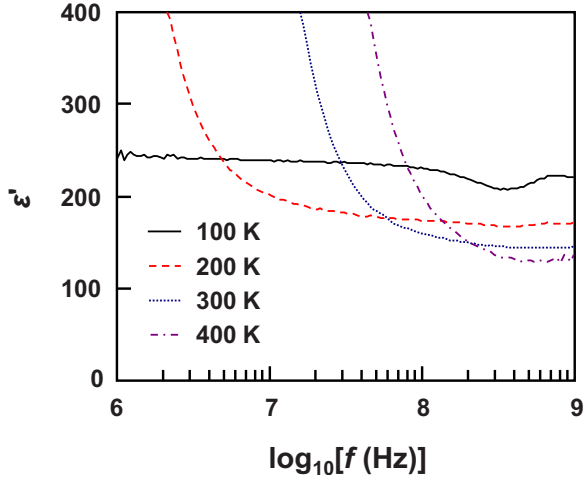
FIG. 2. (Color online) Frequency dependence of ε' at selected temperatures for NBCTO ceramics.

FIG. 3. (Color online) Combined IR and THz reflectivity spectra for NBCTO ceramics at selected temperatures.

tivity data (1 MHz–1 GHz) were obtained using an Agilent 4291B impedance analyzer with a Novocontrol BDS 2100 coaxial sample cell and a Sigma System M18 temperature chamber over the temperature range 100–470 K. IR reflectivity and THz permittivity spectra were obtained at selected temperatures between 9 and 300 K. IR reflectivity measurements were collected using a Fourier transform IR Bruker IFS 113v spectrometer over the frequency range 20–650 cm^{-1} (0.6–19.4 THz) with a liquid He-cooled (1.6 K) Si bolometer detector. In addition, an increased spectral range of 20–3000 cm^{-1} was used to collect the IR reflectivity spectrum at 300 K. Pyroelectric deuterated triglicine sulfate detectors were used for the 300 K measurements. THz permittivity measurements from 5 to 83 cm^{-1} (0.15–2.5 THz) were performed in transmission mode using a time-domain THz spectrometer based on an amplified Ti:sapphire femtosecond laser system. To generate (by optic rectification) and to detect (by electro-optic sampling) the THz pulses, two ZnTe crystal plates were used. Both the transmitted field amplitude and phase shift were simultaneously measured, allowing the direct determination of $\varepsilon^*(\omega)$. To obtain low-temperature spectra, an Oxford Instruments Optistat CF cryostat with thin Mylar windows was used. Finally, THz reflectivity spectra were calculated from directly obtained THz $\varepsilon^*(\omega)$ spectra and, due to the increased accuracy compared to the IR data, were used to normalize the IR reflectivity spectra, with both the normalized IR and THz reflectivity fitted simultaneously. For IR reflectivity and THz transmission measurements, polished pellets of $\sim$8 mm in diameter were used with thicknesses of $\sim$2 mm and 51 μm, respectively.

III. RESULTS AND DISCUSSION

The rf capacitance (10^3–10^6 Hz) and IS measurements (10^1–10^6 Hz) on single-phase NBCTO ceramics have been described briefly in the introduction and presented in detail elsewhere.[19] The frequency dependence of the real component of permittivity ε' for NBCTO ceramics over the fre-

quency range 10^6–10^9 Hz at selected temperatures is shown in Fig. 2. At 100 K, a bulk permittivity plateau in ε' of $\sim$240 is observed over the entire frequency range. Above this temperature, the low-frequency ε' data are observed to increase dramatically due to the IBLC response in NBCTO ceramics, as reported elsewhere.[19] The intrinsic bulk ε_r response is, therefore, only observed at high frequency ($\geq 10^8$ Hz) and increases with decreasing temperature. A more representative view of the bulk permittivity behavior in NBCTO is shown in Fig. 1. At frequencies $\geq 10^8$ Hz, the bulk permittivity is strongly T dependent, increasing with decreasing T from ε' $\sim$ 145 at 300 K to $\sim$220 at 100 K. 1 MHz data obtained from a rf measurement setup in a previous study are included to show the tendency toward a levelling off of ε' (and therefore saturation of ε_r) at low T.[19] A C-W plot of $1/\varepsilon'$ versus T for the 1 GHz data (not shown) was linear over the temperature range 100–200 K with $T_0 \sim -241$ K and $C \sim 75250$ K^{-1}.
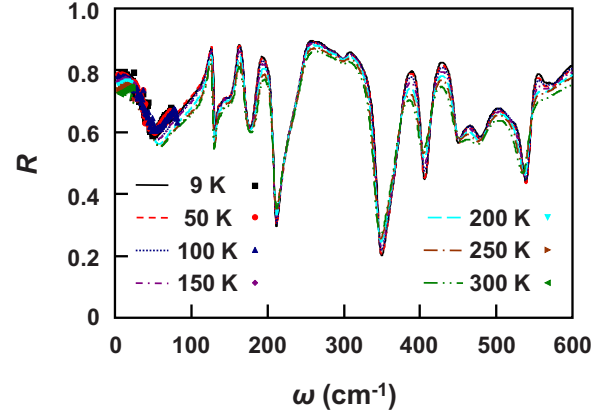
The combined IR and THz reflectivity spectra for NBCTO recorded between 10 and 300 K are shown in Fig. 3. The phonon contribution to the complex permittivity $\varepsilon^*(\omega)$ was determined using IR and THz reflectivity spectra, where the normal reflectivity $R(\omega)$ is related to $\varepsilon^*(\omega)$ by

$$R(\omega) = \left| \frac{\sqrt{\varepsilon^*(\omega)} - 1}{\sqrt{\varepsilon^*(\omega)} + 1} \right|^2, \qquad (3)$$

where ε^* has real and imaginary parts, $\varepsilon^* = \varepsilon' - i\varepsilon''$. Individual phonon parameters were obtained by simultaneously fitting IR and THz spectra using the generalized-oscillator model with the factorized form of the complex permittivity[34]

$$\varepsilon^*(\omega) = \varepsilon_\infty \prod_j \frac{\omega_{\text{LOj}}^2 - \omega^2 + i\omega\gamma_{\text{LOj}}}{\omega_{\text{TOj}}^2 - \omega^2 + i\omega\gamma_{\text{TOj}}}, \qquad (4)$$

where ω_{TOj} and ω_{LOj} denote the transverse and the longitudinal frequencies and γ_{TOj} and γ_{LOj} their corresponding damping constants, respectively, of the jth polar phonon, and ε_∞ represents the high-frequency permittivity resulting from electron-absorption processes. ε' and ε'' components of $\varepsilon^*(\omega)$ spectra were obtained from the fits to IR and THz spectra at various T and are shown in Fig. 4. 22 and 20 phonon modes were used to fit the spectra at 9 K and 300 K,
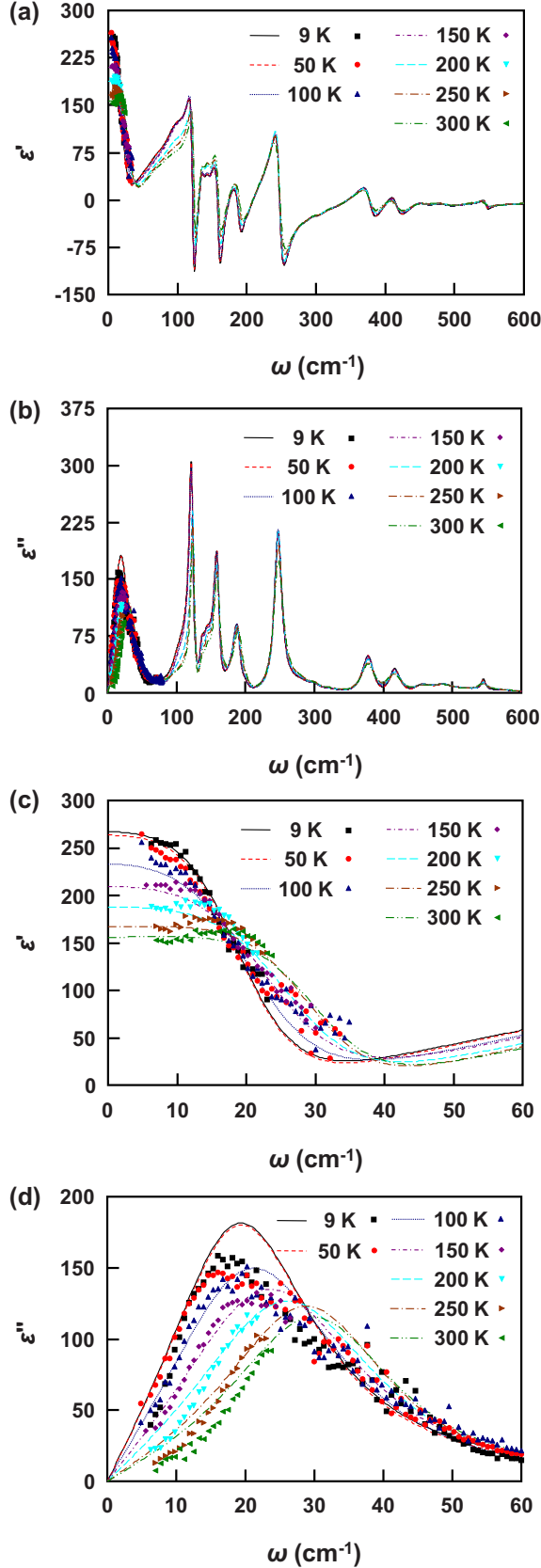
FIG. 4. (Color online) (a) ε' and (b) ε'' at selected temperatures for NBCTO ceramics from IR reflectivity spectra and experimental THz permittivity measurements. (c) and (d) are enlargements of (a) and (b) below 60 cm^{-1}.

respectively. Parameters of the fitted polar phonon modes, including ω_{TOj}, ω_{LOj}, γ_{TOj}, γ_{LOj}, and dielectric strength

$$\Delta\varepsilon_j = \frac{\varepsilon_\infty}{\omega_{TOj}^2} \frac{\prod\limits_{k}(\omega_{LOk}^2 - \omega_{TOj}^2)}{\prod\limits_{k \neq j}(\omega_{TOk}^2 - \omega_{TOj}^2)} \tag{5}$$

at 9 and 300 K are shown in Table I. A ε_∞ of ~6.22 was extracted from the frequency-independent tail above the phonon frequencies in the 300 K reflectivity spectrum and was assumed to be temperature independent.

The only significant phonon frequency shift with T is observed in the lowest frequency mode (soft mode), which is observed at ~34 cm^{-1} in the 300 K spectrum and shifts to ~23 cm^{-1} at 9 K, Fig. 4 and Table I. The shift of all other modes is within ~1%, Figs. 4(a) and 4(b) and Table I. The frequency shift of the soft mode at ~34 cm^{-1} on cooling is observed more clearly in Figs. 4(c) and 4(d), which shows enlargement of ε' and ε'' spectra below 60 cm^{-1}. In particular, the frequency shift of the ε'' peak maximum on cooling is directly visible in Fig. 4(d) and corresponds closely to the fitted soft-mode phonon frequency.

The oscillator strength f_j of each phonon is related to $\Delta\varepsilon_j$ and ω_{TOj} by

$$f_j = \Delta\varepsilon_j \omega_{TOj}^2. \tag{6}$$

For uncoupled phonons the oscillator strength is roughly T independent, therefore each softening of the phonon frequency ω_{TOj} is connected with an increase in $\Delta\varepsilon_j$. The oscillator strength of the lowest frequency mode in NBCTO is T independent within the accuracy of the measurements and data evaluation, indicating limited coupling to any other phonon. The frequency shift of the soft mode, therefore, contributes an increase in ε' from ~96 at 300 K to ~202 at 9 K, Fig. 1 (filled purple triangles) and Table I.

The static permittivity $\varepsilon(0)$ obtained from the fit of the IR reflectivity spectra is defined by

$$\varepsilon(0) = \sum_j \Delta\varepsilon_j + \varepsilon_\infty. \tag{7}$$

From Table I and the y-axis intercept in Fig. 4(c), $\varepsilon(0)$ ~156 and 267 at 300 K and 9 K, respectively, and shows good agreement (Fig. 1, filled green squares) with ε' measured at all T above 100 K with high-frequency coaxial line above 300 MHz and for 1 MHz data recorded below 100 K, Fig. 1. The soft mode almost exclusively accounts for the T dependence of ε'. The frequency dispersion of ε' seen in Fig. 1 at low frequencies and high T is due to the IBLC effect.

The soft-mode frequency ω_{SM} decreases on cooling from 34 cm^{-1} at 300 K and saturates at ~23 cm^{-1} below ~50 K, Fig. 5, representing a frequency shift of 32%. The T dependence of ω_{SM} was fitted to the modified Barrett formula given in Eq. (2), resulting in $B = 2.6(3)$ cm^{-2} K^{-1}, $T_1 = 85(50)$ K, and $T_0 = -155(37)$ K, Fig. 5. From this analysis, quantum fluctuations in NBCTO start near 85 K and the zero-point vibrational energy $[=(k_B T_1)/2$, where k_B is the Boltzmann constant] corresponds very well to the soft-mode

TABLE I. Parameters of the polar phonon modes in NBCTO obtained from the fit of IR and THz spectra at 300 and 9 K. Frequencies ω_{TOj} and ω_{LOj} and dampings γ_{TOj} and γ_{LOj} of modes are in per centimeter, $\Delta\varepsilon_j$ is dimensionless and $\varepsilon_\infty = 6.22$.

No.	300 K					9 K				
	ω_{TOj}	γ_{TOj}	ω_{LOj}	γ_{LOj}	$\Delta\varepsilon_j$	ω_{TOj}	γ_{TOj}	ω_{LOj}	γ_{LOj}	$\Delta\varepsilon_j$
1	33.9	30.8	52.5	25.0	95.9	23.0	27.5	45.3	29.9	202.0
2	71.0	21.8	71.4	22.5	0.6	71.0	20.9	71.4	22.5	0.8
3	100.0	42.6	104.9	45.1	7.6	100.1	32.7	104.9	45.1	9.2
4	123.9	6.4	130.1	3.2	8.3	122.0	7.2	131.0	4.3	12.0
5	135.5	10.6	138.7	13.7	2.2	135.5	8.4	138.7	13.7	1.7
6	144.7	9.5	146.1	11.9	1.0	143.6	9.6	144.7	13.1	0.6
7	159.5	10.2	172.2	12.9	8.2	159.5	8.9	172.2	9.7	8.6
8	191.3	14.6	197.8	10.0	5.8	189.1	13.6	197.8	9.1	6.2
9	198.7	11.4	209.3	6.4	0.6	198.7	10.9	209.3	4.8	0.5
10	247.4	16.6	283.0	42.4	11.1	247.4	13.1	282.6	41.3	10.6
11	287.6	29.6	294.6	25.2	0.6	288.2	28.9	294.5	23.4	0.7
12	301.0	29.6	315.6	34.9	1.2	300.9	28.2	315.6	35.0	1.3
13	321.3	49.7	345.2	12.0	0.8	321.3	51	345.2	8.9	0.8
14	378.2	23.9	400.0	17.1	2.6	378.2	20.1	402.6	9.1	2.8
15	414.3	29.4	444.8	22.3	1.8	415.5	19.3	444.8	15.2	1.6
16	450.6	41.7	475.1	30.9	0.5	450.9	33.0	476.7	24.3	0.5
17	481.7	36.6	533.7	24.8	0.5	482.9	29.9	513.9	29.7	0.4
18						516.0	31.8	539.0	13.1	0.1
19	543.6	19.2	562.3	45.1	0.3	545.0	8.0	568.9	27.4	0.2
20						571.4	14.2	572.4	13.9	0.1
21	566.7	50.3	697.8	46.5	0.2	573.6	27.5	697.8	43.3	0.1
22	719.8	75.6	774.7	50.4	0.1	719.8	75.6	774.7	50.4	0.1

energy $\sim$4 meV ($\equiv\omega_{SM}\sim$34 cm^{-1}) at 300 K. The hypothetical critical temperature (without quantum fluctuations) is near -155 K. $T_1 = 85$ K for NBCTO from this spectroscopic study is now consistent with that reported for other incipient ferroelectrics such as CaTiO$_3$, EuTiO$_3$, and pyrochlore Pb$_{1.83}$Mg$_{0.29}$Nb$_{1.71}$O$_{6.39}$.[4,5,7] The behavior of the soft phonon mode with temperature could also be investigated using
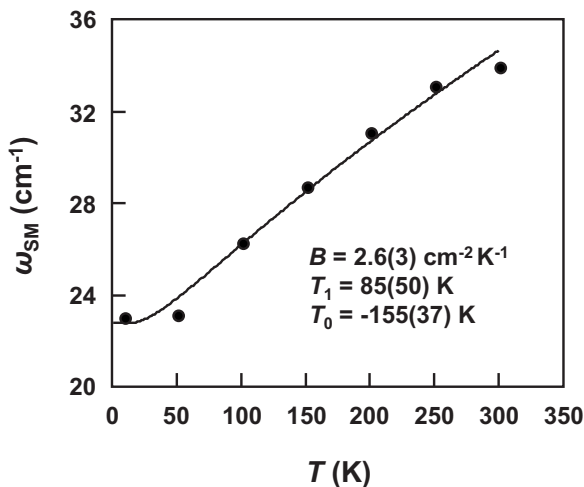
FIG. 5. Fitting (solid line) of the soft-mode frequency ω_{SM} with T according to the modified Barrett formula [Eq. (2) in text].

hyper-Raman scattering, which could provide additional supporting data about the incipient ferroelectric behavior in NBCTO.

Homes *et al.*[15] observed ten T_u symmetry polar phonons in the IR spectrum of CCTO, which is in good agreement with a first-principles study and factor group analysis of lattice dynamics in $Im\bar{3}$ space group.[35] However, we have observed 22 modes at 9 K and 20 at 300 K (see Table I) for NBCTO, although NBCTO is known to crystallize in the same $Im\bar{3}$ space group as CCTO.[36] The expected lattice dynamics of NBCTO have recently been calculated using density-functional theory within the spin-density approximation.[37] The calculation was performed in the primitive cubic space group $Pm\bar{3}$. 20 polar modes are expected from the calculation, including a low-frequency soft mode $\sim$50 cm^{-1} which involves the antiparallel motion of Na and Bi ions as a group against Cu and O atoms. The $Pm\bar{3}$ model assumes ordering of Na and Bi ions, however, our Rietveld refinement on experimental neutron-diffraction data refines in body-centered-cubic symmetry, space group $Im\bar{3}$, at 300 K, with the symmetry being retained down to 4 K.[36] The refined model based on the experimental diffraction data shows Na and Bi ions on the A site to be disordered over the long range. IR spectroscopy is extremely sensitive to local crystal structure and, therefore, short-range ordering of Na and Bi ions cannot be discounted. Short-range ordering in

NBCTO could account for the additional observed phonon modes compared to CCTO and the similar number of phonon modes as calculated for space group $Pm\bar{3}$. However, it cannot be discounted that the additional phonon modes in NBCTO are due to the presence of two cations with different mass, Na and Bi, on the *A* site, causing splitting of the 10 phonon modes observed for CCTO.

In a previous IR study of NBCTO, 10 polar phonon modes were observed at room temperature.[38] The lowest frequency mode reported was ~ 121 cm^{-1} and $\varepsilon(0) \sim 54$. The lack of a mode <100 cm^{-1} and the very low $\varepsilon(0)$ value compared to the values obtained in this study using both IR and rf measurements makes it difficult to compare with their results.

A soft phonon mode is observed in the IR spectrum for CdCu$_3$Ti$_4$O$_{12}$ (CdCTO), with $\omega \sim 75$ cm^{-1} at 295 K (66 cm^{-1} at 10 K),[39] whereas the lowest frequency phonon mode for CCTO occurs with $\omega \sim 122$ cm^{-1} at 295 K (116 cm^{-1} at 10 K).[15] 11 polar phonons were observed for CdCTO confirming the same $Im\bar{3}$ structure as in CCTO.[39] A lower soft-mode frequency is expected for CdCTO due to the higher mass of Cd compared to Ca. Lattice-dynamic calculations[40] have shown the mode at 122 cm^{-1} in both CCTO and CdCTO, dominated primarily by Cu-O motion, to be largely unaffected by the replacement of Ca by Cd on the *A* site, due to the similar size and nominal valence of these ions. In addition, the lowest frequency mode with $\omega \sim 75$ cm^{-1} for CdCTO was shown to correspond to a higher frequency mode with $\omega \sim 141$ cm^{-1} for CCTO. The softening of this mode to <100 cm^{-1} for CdCTO could not be completely accounted for by the difference in mass between Ca^{2+} and Cd^{2+} ions. Chemical-bonding effects associated with the presence of the $4d^{10}$ electronic shell in the Cd^{2+} ions were suggested to play a significant role in the degree of softening for the lowest frequency mode in CdCTO.

The lattice-dynamic calculations for NBCTO, although possessing ordering of Na and Bi ions, showed a lowering of the soft-mode frequency for NBCTO (predicted at ~ 50 cm^{-1}) (Ref. [37]) compared to CCTO (122 cm^{-1}).[15,39] The predicted value of the soft mode for ordered NBCTO is close to the experimentally measured value of ~ 34 cm^{-1}. It is possible, although speculative, that the mode at 34 cm^{-1} and a higher frequency mode, possibly one of ~ 71, 100, 124, or 136 cm^{-1}, in NBCTO could be due to the mixed occupancy of Na$^+$ and Bi^{3+} ions on the *A* site, where the difference in mass causes a splitting of the phonon and that chemical bonding and/or steric effects associated with the electron lone pair on the Bi$^{3+}(6s^2)$ ions cause further softening of the lowest mode to 34 cm^{-1}. Chemical bonding/steric effects involving the *A* site have been suggested to occur in CCTO. A total scattering structural study found the atomic displacement parameters of Ca and Cu ions to have an unusual temperature dependence with modeling based on bond-valence concepts suggesting that underbonding of Ca ions at low temperature may result in slight off-center *A*-site displacements.[41] It is clear more in-depth experimental and computational studies on NBCTO and other members of the ACu$_3$Ti$_4$O$_{12}$ family are now required to provide a better understanding of the intrinsic relationships between the structural, vibrational, and lattice dielectric properties of this family of compounds.

In conclusion, we have shown that the giant extrinsic ε' due to the IBLC mechanism in NBCTO does not extend to frequencies above 300 MHz. The intrinsic ε' of NBCTO increases on cooling and saturates at low temperatures, behavior associated with incipient ferroelectricity. IR and THz spectra reveal a soft polar optic mode which is responsible for the high and *T*-dependent intrinsic permittivity of NBCTO. A combination of the levelling off of ε' at low *T* and fitting of the *T* dependence of the soft-mode frequency to a modified Barrett formula [Eq. (2)] confirms incipient ferroelectricity in NBCTO. Such electrical behavior is consistent with that expected for a heavily TiO$_3$ tilted unusual variant of the perovskite structure with centrosymmetric symmetry.

[1] J. H. Barrett, Phys. Rev. **86**, 118 (1952).

[2] K. A. Müller and H. Burkard, Phys. Rev. B **19**, 3593 (1979).

[3] G. A. Samara and B. Morosin, Phys. Rev. B **8**, 1256 (1973).

[4] V. V. Lemanov, A. V. Sotnikov, E. P. Smirnova, M. Weihnacht, and R. Kunze, Solid State Commun. **110**, 611 (1999).

[5] S. Kamba, D. Nuzhnyy, P. Vaněk, M. Savinov, K. Knížek, Z. Shen, E. Šantavá, K. Maca, M. Sadowski, and J. Petzelt, EPL **80**, 27002 (2007).

[6] P. H. Sun, T. Nakamura, Y. J. Shan, Y. Inaguma, and M. Itoh, Ferroelectrics **200**, 93 (1997).

[7] S. Kamba, D. Nuzhnyy, S. Denisov, S. Veljko, V. Bovtun, M. Savinov, J. Petzelt, M. Kalnberga, and A. Sternberg, Phys. Rev. B **76**, 054125 (2007).

[8] W. Kleemann, J. Dec, Y. G. Wang, P. Lehnen, and S. A. Prosandeev, J. Phys. Chem. Solids **61**, 167 (2000).

[9] J. G. Bednorz and K. A. Müller, Phys. Rev. Lett. **52**, 2289 (1984).

[10] V. V. Shvartsman, S. Bedanta, P. Borisov, W. Kleemann, A. Tkach, and P. M. Vilarinho, Phys. Rev. Lett. **101**, 165704 (2008).

[11] G. A. Samara, in *Solid State Physics*, edited by H. Ehrenreich and F. Spaepen (Academic, San Diego, 2001), Vol. 56, pp. 240–458.

[12] O. E. Kvyatkovskii, Phys. Solid State **43**, 1401 (2001).

[13] Y. Minaki, M. Kobayashi, Y. Tsujimi, T. Yagi, M. Nakanishi, R. Wang, and M. Itoh, J. Korean Phys. Soc. **42**, S1290 (2003).

[14] M. A. Subramanian, D. Li, N. Duan, B. A. Reisner, and A. W. Sleight, J. Solid State Chem. **151**, 323 (2000).

[15] C. C. Homes, T. Vogt, S. M. Shapiro, S. Wakimoto, and A. P. Ramirez, Science **293**, 673 (2001).

[16] M. A. Subramanian and A. W. Sleight, Solid State Sci. **4**, 347 (2002).

[17] D. C. Sinclair, T. B. Adams, F. D. Morrison, and A. R. West, Appl. Phys. Lett. **80**, 2153 (2002).

[18] J. Liu, C. G. Duan, W. N. Mei, R. W. Smith, and J. R. Hardy, J. Appl. Phys. **98**, 093703 (2005).

[19] M. C. Ferrarelli, T. B. Adams, A. Feteira, D. C. Sinclair, and A. R. West, Appl. Phys. Lett. **89**, 212904 (2006).

[20] J. Sebald, S. Krohns, P. Lunkenheimer, S. G. Ebbinghaus, S. Riegg, A. Reller, and A. Loidl, Solid State Commun. **150**, 857 (2010).

[21] B. Bochu, J. Chenavas, J. C. Joubert, and M. Marezio, J. Solid State Chem. **11**, 88 (1974).

[22] B. Bochu, M. N. Deschizeaux, J. C. Joubert, A. Collomb, J. Chenavas, and M. Marezio, J. Solid State Chem. **29**, 291 (1979).

[23] Y. Ozaki, M. Ghedira, J. Chenavas, J. C. Joubert, and M. Marezio, Acta Crystallogr., Sect. B: Struct. Crystallogr. Cryst. Chem. **33**, 3615 (1977).

[24] Y. Shimakawa, Inorg. Chem. **47**, 8562 (2008).

[25] Y. W. Long, N. Hayashi, T. Saito, M. Azuma, S. Muranaka, and Y. Shimakawa, Nature (London) **458**, 60 (2009).

[26] S. Y. Chung, I. D. Kim, and S. J. L. Kang, Nature Mater. **3**, 774 (2004).

[27] S. V. Kalinin, J. Shin, G. M. Veith, A. P. Baddorf, M. V. Lobanov, H. Runge, and M. Greenblatt, Appl. Phys. Lett. **86**, 102902 (2005).

[28] P. Fiorenza, R. Lo Nigro, C. Bongiorno, V. Raineri, M. C. Ferrarelli, D. C. Sinclair, and A. R. West, Appl. Phys. Lett. **92**, 182907 (2008).

[29] M. C. Ferrarelli, D. C. Sinclair, A. R. West, H. A. Dabkowska, A. Dabkowski, and G. M. Luke, J. Mater. Chem. **19**, 5916 (2009).

[30] S. Krohns, P. Lunkenheimer, S. G. Ebbinghaus, and A. Loidl, J. Appl. Phys. **103**, 084107 (2008).

[31] M. Li, A. Feteira, D. C. Sinclair, and A. R. West, Appl. Phys. Lett. **88**, 232903 (2006).

[32] M. Li, A. Feteira, D. C. Sinclair, and A. R. West, Appl. Phys. Lett. **91**, 132911 (2007).

[33] M. C. Ferrarelli, D. C. Sinclair, and A. R. West, Appl. Phys. Lett. **94**, 212901 (2009).

[34] F. Gervais, in *Infrared and Millimeter Waves*, edited by K. J. Button (Academic, New York, 1983), Vol. 8, Chap. 7, p. 279.

[35] L. He, J. B. Neaton, M. H. Cohen, D. Vanderbilt, and C. C. Homes, Phys. Rev. B **65**, 214112 (2002).

[36] M. C. Ferrarelli, Ph.D. thesis, University of Sheffield, 2009.

[37] C. Parlak and R. Eryiğit, J. Phys.: Condens. Matter **20**, 175220 (2008).

[38] K. C. Liang, H. L. Liu, H. D. Yang, W. N. Mei, and D. C. Ling, J. Phys.: Condens. Matter **20**, 275238 (2008).

[39] C. C. Homes, T. Vogt, S. M. Shapiro, S. Wakimoto, M. A. Subramanian, and A. P. Ramirez, Phys. Rev. B **67**, 092106 (2003).

[40] L. He, J. B. Neaton, D. Vanderbilt, and M. H. Cohen, Phys. Rev. B **67**, 012103 (2003).

[41] E. S. Božin, V. Petkov, P. W. Barnes, P. M. Woodward, T. Vogt, S. D. Mahanti, and S. J. L. Billinge, J. Phys.: Condens. Matter **16**, S5091 (2004).